

# Tunable multi-wavelength filter in periodically poled LiNbO<sub>3</sub> by a local-temperature-control technique

Jinghe Wang, Jianhong Shi\*, Zhuoer Zhou, Xianfeng Chen\*\*

*Institute of Optics & Photonics, Department of Physics, The State Key Laboratory on Fiber-Optic Local Area Network and Advanced Optical Communication Systems, Shanghai Jiaotong University, 800 Dongchuan Road, Shanghai 200240, China*

\*[purewater@sjtu.edu.cn](mailto:purewater@sjtu.edu.cn) \*\*[xfchen@sjtu.edu.cn](mailto:xfchen@sjtu.edu.cn)

**Abstract:** A tunable multi-wavelength filter can be realized in periodically poled LiNbO<sub>3</sub> by using a local-temperature-control technique. In this paper, a tunable single-wavelength and double-wavelength filter of this kind is experimentally demonstrated. In our experiment, the output transmissivity peaks of the filter can be tuned to any wavelengths by properly setting the local temperature distribution along the sample. The dependence between the wavelength shift and temperature change is  $\Delta\lambda/\Delta T \approx -0.598 \text{ nm}/^\circ\text{C}$ . The wavelength tuning range of such filter is determined by the tuning range of the temperature control device according to this  $\Delta\lambda/\Delta T$  relation.

©2007 Optical Society of America

OCIS codes: (120.2440) Filters; (260.1440) Birefringence; (160.3730) Lithium niobate

---

## References and links

1. R. L. Byer, "Quasi-phase matched nonlinear interactions and devices," *J. Nonlin. Opt. Phys. Mater.* **6**, 549-592 (1997).
2. L. E. Myers, R. C. Eckardt, M. M. Fejer, R. L. Byer, W. R. Bosenberg, and J. W. Pierce, "Quasi-phase-matched optical parametric oscillation in bulk periodically poled LiNbO<sub>3</sub>," *J. Opt. Soc. Am. B* **12**, 2102-2116 (1995).
3. K. Mizuuchi and K. Yamamoto, "Waveguide second-harmonic generation device with broadened flat quasi-phase-matching response by use of a grating structure with located phase shifts," *Opt. Lett.* **23**, 1880-1882 (1998).
4. Y. Q. Lu, Z. L. Wan, Q. Wang, Y. X. Xi, and N. B. Ming, "Electro-optic effect of periodically poled optical superlattice LiNbO<sub>3</sub> and its applications," *Appl. Phys. Lett.* **77**, 3719-3721 (2000).
5. X. F. Chen, J. H. Shi, Y. P. Chen, Y. M. Zhu, Y. X. Xia, and Y. L. Chen, "Electro-optic Solc-type wavelength filter in periodically poled lithium niobate," *Opt. Lett.* **28**, 2115-2117 (2003).
6. J. H. Shi, X. F. Chen, Y. P. Chen, Y. M. Zhu, Y. X. Xia, Y. L. Chen, "Observation of Solc-like filter in periodically poled lithium niobate," *Electron. Lett.* **39**, 224-225 (2003).
7. L. J. Chen, J. H. Shi, X. F. Chen, and Y. X. Xia, "Photovoltaic effect in a periodically poled lithium niobate Solc-type wavelength filter," *Appl. Phys. Lett.* **88**, 1211118 (2006).
8. Y. M. Zhu, X. F. Chen, J. H. Shi, Y. P. Chen, Y. X. Xia, and Y. L. Chen, "Wide-range tunable wavelength filter in periodically poled lithium niobate," *Opt. Commun.* **228**, 139-143 (2003).
9. D. H. Jundt, "Temperature-dependent Sellmeier equation for the index of refraction,  $n_e$ , in congruent lithium niobate," *Opt. Lett.* **22**, 1553-1555 (1997).
10. Y. L. Lee, Y. Noh, C. Jung, T. J. Yu, B. Yu, J. Lee, and D. Ko, "Reshaping of a second-harmonic curve in periodically poled Ti: LiNbO<sub>3</sub> channel waveguide by a local-temperature-control technique," *Appl. Phys. Lett.* **86**, 011104 (2005).
11. A. Yariv and P. Yeh, *Optical Waves in Crystal: Propagation and Control of Laser Radiation* (John Wiley & Sons, New York, 1984), Chap. 5.

---

## 1. Introduction

Periodically poled LiNbO<sub>3</sub> (PPLN) was extensively studied in the past decade for its outstanding nonlinear optical properties. Because the nonlinear coefficient changes sign periodically due to the periodic reversal of the ferroelectric domains in PPLN, quasi phase

matching (QPM) occurs during the frequency conversion process [1-3]. Many nonlinear optical applications, including second-harmonic generation and optical parametric oscillation have been demonstrated in PPLN. In addition to the nonlinear coefficient, the electro-optical (EO) coefficient is also periodically modulated due to the periodic domain inversion of the PPLN, which results in some interesting EO properties. An EO Solc-type filter can be realized by applying an external electric field to the PPLN along the transverse (Y) axis, causing an azimuth angle deviation alternatively positive and negative from the spontaneous polarization directions in different domains as they are periodically modulated [4,5]. It is also observed that even without the applied electric field, the Solc-type filter still exists in PPLN, which indicates that there should be a small angle between the optical axes of the positive domains and the negative domains after the room temperature electric poling process [6, 7].

In a PPLN Solc-type filter, the central wavelength is determined by the period of the domain inversion and the ordinary and extraordinary refractive indices. Since the indices are temperature dependent, the central wavelength of such filter can be shifted by changing the working temperature of the whole PPLN [8, 9]. If we apply a temperature distribution along the PPLN through a local-temperature-control technique that is being used to control and reshape the second harmonic (SH) curve in a periodically poled Ti:LiNbO<sub>3</sub> (Ti:PPLN) waveguide [10], then the PPLN will be divided into several temperature sections and each section will give a central wavelength determined by its local temperature. By combining the contributions from all the temperature sections in the PPLN, a multi-wavelength filter can be realized. By properly controlling the temperature of each section, we can construct a tunable multi-wavelength filter for any wavelength according to the practical needs of different applications.

In this paper, we experimentally demonstrated a tunable single-wavelength and double-wavelength filter with a two-section pattern temperature distribution realized by using a local-temperature-control technique and then showed its agreement with theoretical calculations.

## 2. Theory of tunable PPLN multi-wavelength filter

By applying an external electric field along the Y axis to a Z-cut lithium niobate crystal, the refractive index ellipsoid deforms and consequently the Y and Z axes of the lithium niobate rotate by a small angle  $\theta$  about the X axis [4, 11]. Owing to the periodically reversed domain structure of PPLN, the rotation angle  $\theta$  changes sign alternately positive and negative within the non-inverted and inverted domains. With two crossed polarizers placed at the two ends of the PPLN, a folded Solc-type filter is easily formed [5]. In such a structure, each domain in the PPLN works as a half-wave plate. As reported, even without applying an external electric field, the Solc-type filter will still exist in PPLN [6, 7]. The central wavelength of this filter is determined by Eq. (1) [11]:

$$\lambda_v = \frac{1}{2v+1}(n_o - n_e)\Lambda, \quad v=0,1,2\dots, \quad (1)$$

where  $v$  is the order of the half-wave plate and equals to zero in this application,  $n_o$  and  $n_e$  are the ordinary and extraordinary refractive indices respectively, and  $\Lambda$  is the period of PPLN giving the sum length of one positive domain and one negative domain. The corresponding full width at half maximum (FWHM) of this filter can be estimated by Eq. (2) [11]:

$$\Delta\lambda_{1/2} = 1.60\lambda_0 / N, \quad (2)$$

where  $N$  is the number of all the domains and  $\lambda_0$  is the central wavelength.

Since the refractive indices are temperature dependent, when we change the working temperature of the PPLN, the  $(n_o - n_e)$  part in Eq. (1) will consequently change, thus the central wavelength will be tuned to a new value. The temperature dependent Sellmeier equation for lithium niobate is given by Eq. (3) [9]:

$$n^2 = A_1 + \frac{A_2 + B_1 F}{\lambda^2 - (A_3 + B_2 F)^2} + B_3 F - A_4 \lambda^2 \quad (3)$$

where  $F=(T-24.5)(T+570.5)$ ,  $T$  is the temperature in Celsius scale, and  $A_{1-4}$  and  $B_{1-3}$  are constant parameters. From Eq. (1) we can also derive the relationship between the wavelength shift and temperature change, which can be expressed by Eq. (4):

$$\frac{d\lambda}{dT} = \Lambda \times \left( \frac{dn_o(\lambda, T)}{dT} - \frac{dn_e(\lambda, T)}{dT} \right) \quad (4)$$

For example, for the 21 $\mu$ m period in a PPLN sample within a relatively narrow temperature range around room temperature, the theoretically calculated dependence shows  $d\lambda/dT=-0.588\text{nm}/^\circ\text{C}$  [8].

We can also apply a temperature distribution along the PPLN using a local-temperature-control technique, which divides the PPLN into several sections each with a different temperature [10]. In this case, every section can be viewed as a Solc-type filter working under its local temperature and contributes a central wavelength according to Eq. (1). Together with all the temperature sections in the sample, a multi-wavelength filter is realized. Since every central wavelength is tunable by changing the local temperature of each section, if we apply temperature control units to control the temperature distribution along the sample, a tunable multi-wavelength filter can be constructed in PPLN.

### 3. Experimental results and discussions

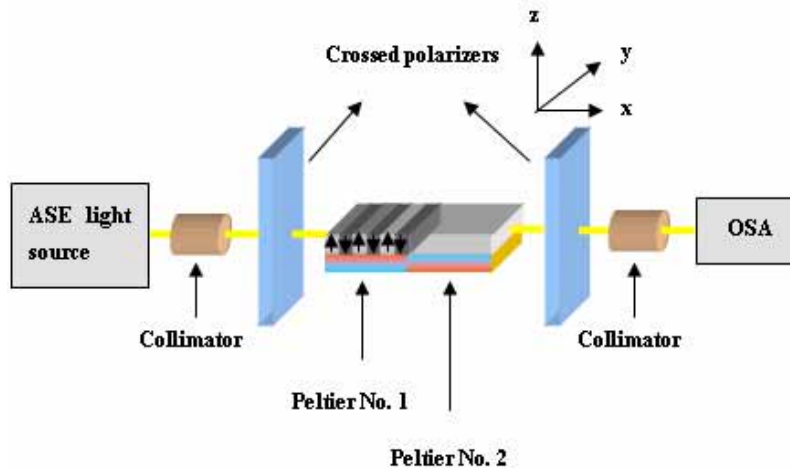


Fig. 1. The schematic diagram of the experimental setup

The schematic diagram of the experiment is shown in Fig. 1. A PPLN crystal is placed between two crossed polarizers. The polarization of the front (end) polarizer is along the Y (Z) axis. The arrows inside the PPLN indicate the spontaneous polarization directions. The PPLN is fabricated by the electric field poling technique at room temperature. The sample with a dimension of 41.15(L) $\times$ 10(W) $\times$ 0.5(T)mm<sup>3</sup> consists of nine gratings with periods from 20 $\mu$ m to 22 $\mu$ m and a width of 1mm. We use the EXFO optical test system in our experiment, which includes a broadband ASE source with an output wavelength range from approximately 1530nm to 1560nm, as well as an optical spectrum analyzer (OSA). To obtain the localized temperature in PPLN, two Peltier devices are placed under the sample. The temperatures of the two sections are controlled by temperature control units.

First, the two Peltiers are both at the room temperature 23.5 $^\circ\text{C}$  and then shifted to 15.2 $^\circ\text{C}$ . The normalized transmission spectra of the 21.0 $\mu$ m period measured by OSA are shown in Fig. 2 using symbol points. As the temperature changed, the central wavelength shifted from 1542.192nm at the room temperature (red symbol points) to 1546.992nm at 15.2 $^\circ\text{C}$

(blue symbolled points), and the measured FWHM was approximately 0.68nm. We can see that with this one-section pattern temperature distribution, the PPLN does work as a Solc-type filter, even without an electric field applied in the Y axis. The sky-blue and pink solid curves are the theoretical transmission spectra of the filter using the temperature dependent Sellmeier equation given in Eq. (3). The experimental and theoretical results are in agreement with each other in shape, but there is a difference in the transmission peak between them that may arise from the unknown data of the wavelength and temperature dependencies of the refractive index of our PPLN sample. Because the  $n_o$  and  $n_e$  always appears as  $(n_o-n_e)$ , we only choose the  $A_1$  parameter of  $n_e$  in the Sellmeier equation given in Eq. (3) to make a correction, changing its value from 4.9048 to 4.9057 in order to describe our sample better. The black and green solid curves are theoretical simulations using this new  $A_1$  parameter. For such a correction, the experimental and theoretical results are in agreement. In the later theoretical simulations, we always use this new  $A_1$  value and use solid lines to represent all the calculated results. Since it is proven that the rotation angle ( $\pm\theta$ ) of the optical axes in the positive and negative domains mainly determine the peak transmissivity value, in our calculation we have properly adjusted  $|\pm\theta|$  to make the peak transmissivity value equal to one in order to compare the experimental and theoretical results clearly [7].

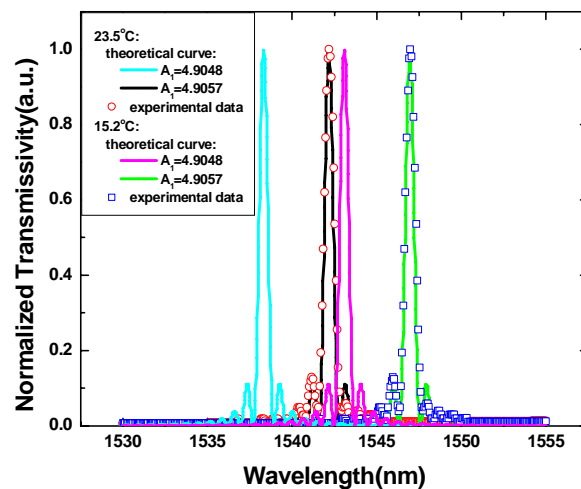


Fig. 2. Tunable single-wavelength filter realized in PPLN by setting the two Peltier devices at the same temperature. The symbolled points at left (right) are the measured peak of the filter at 23.50°C (15.20°C), and the central wavelength is 1542.192nm (1546.992nm). The solid curves with the  $A_1$  parameter equal to 4.9048 (4.9057) show the theoretical simulations before (after) the correction for  $A_1$ .

We then set the Peltier No. 1 to a warmer temperature and the Peltier No. 2 to a cooler temperature. Thus the PPLN was divided into two temperature sections. First we heated the Peltier No. 1 and cooled the Peltier No. 2 almost equally from the room temperature 23.5°C to 26.1°C and 21.2°C respectively. The normalized transmission spectra for the 21.0 $\mu$ m period measured by OSA is shown in the first figure in Fig. 3 using symbolled points. The corresponding double peaks appeared close to each other at the central wavelengths 1540.616nm and 1543.63nm respectively, and almost symmetrical at around the room-temperature central wavelength 1542.192nm (blue symbolled points). This result shows that by applying a two-section pattern temperature distribution to the sample, the PPLN can become a double-wavelength filter.

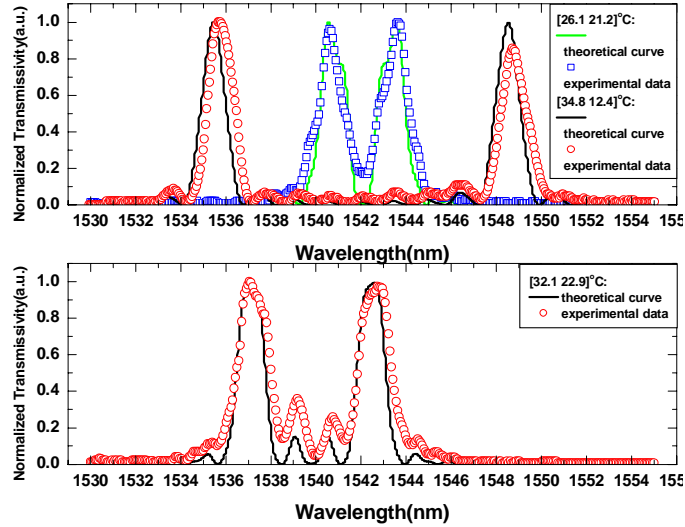


Fig. 3. Tunable double-wavelength filter realized in PPLN by applying a two-section pattern temperature distribution along the sample. In the first figure, under a [26.1 21.2] °C pattern temperature distribution, the double peaks were at 1540.616nm and 1543.63nm, and under a [34.8 12.4] °C pattern temperature distribution, the double peaks were tuned to 1538.562nm and 1545.6845nm, for the symmetrical case. In the second figure, under a [32.1 22.9] °C pattern temperature distribution, the double peaks were set to 1537.078nm and 1542.763nm, for the arbitrary case.

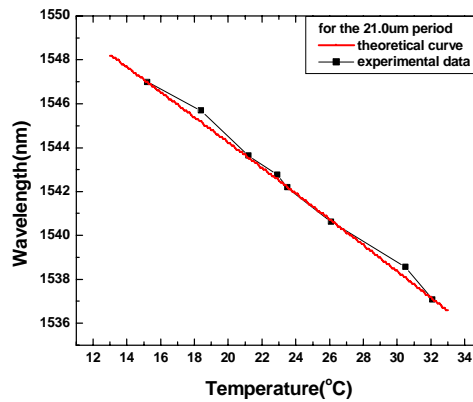


Fig.4. The relationship between the central wavelength of the filter and the working temperature. The symboled line is the experimental measurement, and the solid line represents the theoretical calculation from Eq. (3) but with the new  $A_1$  parameter after our correction.

We then set a larger temperature difference between the two sections, but again kept the temperature change of both sections almost equal. This time we set the temperature for the heated section to 34.8°C and for the cooled section to 12.4°C. The measured transmission spectra is shown with the red symbolled points in the first figure in Fig. 3. The double peaks were tuned away from each other showing up at 1535.608nm and 1548.686nm respectively but still almost symmetrical at around the room-temperature central wavelength 1542.192nm. So under a temperature change, the double-wavelength filter can be tunable. For this double-wavelength case, the measured FWHM is about 1.5nm.

We can also tune the double peaks arbitrarily to any wavelengths away from the room-temperature single peak by properly setting the temperature distribution, which will be important for future applications. For example, we can have double peaks at 1537.078nm and 1542.763nm with a heated section of 32.1°C and a cooled section of 22.9°C (see the second figure in Fig. 3). The measured FWHM is again about 1.5nm.

Comparing our experimental results with all the theoretical simulations, we find both in agreement with each other in terms of shape. For the PPLN used in our experiment, the period is 21.0μm and the domain number is about 3919. Theoretically we have  $\Delta\lambda_{1/2}=1.60\lambda_0/N\approx 0.63\text{nm}$  for the single-wavelength case and  $\Delta\lambda_{1/2}=1.60\lambda_0/(N/2)\approx 1.3\text{nm}$  for the double-wavelength case. The experimental FWHMs are 0.68nm and 1.5nm, respectively. They also agreed well with the theoretically estimated FWHMs.

The symbolized line in Fig. 4 shows the experimentally measured central wavelength shift versus the temperature change. We can see that the relationship between them is almost linear and  $\Delta\lambda/\Delta T$  is approximately  $-0.598\text{nm}/^\circ\text{C}$ . The solid line in Fig. 4 gives the theoretically calculated value from the Sellmeier equation given in Eq.(3) with the new corrected  $A_1$  parameter. The experimental results are in agreement with the theoretical simulation as well. Within a temperature range only limited by the temperature control device, and according to the measured dependence between the wavelength shift and temperature change, we can realize a corresponding wavelength tuning range for this kind of filter. And in such a wavelength range, the output transmission peaks can be tuned to any needed wavelengths by properly controlling the temperature distribution according to future applications.

#### 4. Conclusion

We demonstrated a tunable single-wavelength filter and double-wavelength filter realized in PPLN by applying a temperature distribution along the sample, and observed a dependence between the wavelength shift and the temperature change of  $-0.598\text{nm}/^\circ\text{C}$ . Utilizing a similar structure, a tunable multi-wavelength filter can also be realized as predicted by theory, and this kind of filter is tunable in a wavelength range only limited by the temperature tuning range of the temperature control device. We believe this kind of multi-wavelength filter tuned by temperature will have potential applications in the dense wavelength division multiplexer (DWDM) optical fiber communication system where it can be employed for all-optical wavelength routing.

#### Acknowledgments

This research was supported by the National Natural Science Foundation of China (No. 60508015, No.60477016 and No.10574092, the Foundation for Development of Science and Technology of Shanghai (04DZ14001) and the Excellent Young Teachers Program of MOE, P. R. C.